

## Fullerenes

International Edition: DOI: 10.1002/anie.201900983  
German Edition: DOI: 10.1002/ange.201900983First Synthesis and Characterization of CH<sub>4</sub>@C<sub>60</sub>

Sally Bloodworth, Gabriela Sitinova, Shamim Alom, Sara Vidal, George R. Bacanu, Stuart J. Elliott, Mark E. Light, Julie M. Herniman, G. John Langley, Malcolm H. Levitt, and Richard J. Whitby\*

**Abstract:** The endohedral fullerene CH<sub>4</sub>@C<sub>60</sub> in which each C<sub>60</sub> fullerene cage encapsulates a single methane molecule, has been synthesized for the first time. Methane is the first organic molecule, as well as the largest, to have been encapsulated in C<sub>60</sub> to date. The key orifice contraction step, a photochemical desulfinylation of an open fullerene, was completed, even though it is inhibited by the endohedral molecule. The crystal structure of the nickel(II) octaethylporphyrin/benzene solvate shows no significant distortion of the carbon cage, relative to the C<sub>60</sub> analogue, and shows the methane hydrogens as a shell of electron density around the central carbon, indicative of the quantum nature of the methane. The <sup>1</sup>H spin-lattice relaxation times (T<sub>1</sub>) for endohedral methane are similar to those observed in the gas phase, indicating that methane is freely rotating inside the C<sub>60</sub> cage. The synthesis of CH<sub>4</sub>@C<sub>60</sub> opens a route to endofullerenes incorporating large guest molecules and atoms.

Soon after the discovery of C<sub>60</sub> in 1985,<sup>[1]</sup> came recognition that its approximately spherical 3.7 Å diameter cavity provides a unique environment in which to isolate single atoms.<sup>[2]</sup> Since then endohedral fullerenes, that is, compounds denoted A@C<sub>60</sub> in which molecules or atoms are enclosed within the fullerene cage, have been the focus of substantial experimental and theoretical efforts.<sup>[3–5]</sup> Endohedral fullerenes may be synthesized by forming the fullerene in the presence of the endohedral species (particularly successful for metallofullerenes),<sup>[3,5]</sup> by high temperature and pressure treatment of the fullerene with the endohedral species (inert gas@C<sub>60</sub>),<sup>[6,7]</sup>

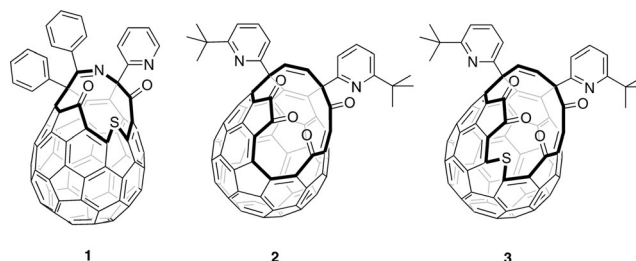


**Figure 1.** Open-cage fullerenes. Preparation of H<sub>2</sub>@C<sub>60</sub> from **1**, and of H<sub>2</sub>O@C<sub>60</sub> and HF@C<sub>60</sub> from **2**, is known; as are a series of open-cage derivatives A@**3**.

or by ion bombardment of the fullerene (N@C<sub>60</sub>),<sup>[8]</sup> but all give very low incorporation and require extensive purification. Furthermore, these methods are not applicable to the incorporation of small organic molecules.

The macroscopic-scale preparation of endohedral fullerenes by multi-step “molecular surgery”<sup>[9–12]</sup> involves chemically opening an orifice in the fullerene, of a size suitable to allow entry of the single molecule. Suture of this orifice to restore the pristine carbon cage was pioneered by Komatsu<sup>[13,14]</sup> and Murata<sup>[15]</sup> who reported the first syntheses of H<sub>2</sub>@C<sub>60</sub> and H<sub>2</sub>O@C<sub>60</sub> following insertion of H<sub>2</sub> or H<sub>2</sub>O under high-pressure, into open-cage fullerenes **1** and **2**, respectively. Optimized procedures for the synthesis of H<sub>2</sub>@C<sub>60</sub> and H<sub>2</sub>O@C<sub>60</sub> have subsequently been reported by ourselves,<sup>[16]</sup> based on Murata’s open-cage C<sub>60</sub> derivative **2**, and also applied to the synthesis of HF@C<sub>60</sub> (Figure 1).<sup>[17,18]</sup>

The macroscopic quantities of endohedral fullerenes provided by molecular surgery have allowed detailed investigation of physical properties, including by neutron scattering, infrared spectroscopy, and NMR spectroscopy.<sup>[19]</sup> These methods have shown that, as a result of the inert and highly symmetrical environment of the cavity, an entrapped molecule behaves much as would be expected in the very low-pressure gas state,<sup>[17,19–23]</sup> displaying free rotation at cryogenic temperatures.<sup>[19–24]</sup>

The 16-membered orifice of **2** is too small to allow entry of bigger guests, but these can be accommodated by the larger (17-membered) opening of fullerene **3**.<sup>[25]</sup> Insertion of N<sub>2</sub> and CO<sub>2</sub>,<sup>[26]</sup> CH<sub>3</sub>OH and H<sub>2</sub>CO,<sup>[27]</sup> CH<sub>4</sub> and NH<sub>3</sub>,<sup>[28]</sup> NO,<sup>[29]</sup> and O<sub>2</sub>,<sup>[30]</sup> into **3** have all been recently described, but a procedure for suturing the opening of A@**3** to give A@C<sub>60</sub> has not yet been reported. In this article, we describe the successful closure of A@**3** to give A@C<sub>60</sub>.

The endohedral fullerenes H<sub>2</sub>@C<sub>60</sub> and H<sub>2</sub>O@C<sub>60</sub> are exceptional platforms for the study of nuclear spin isomer-

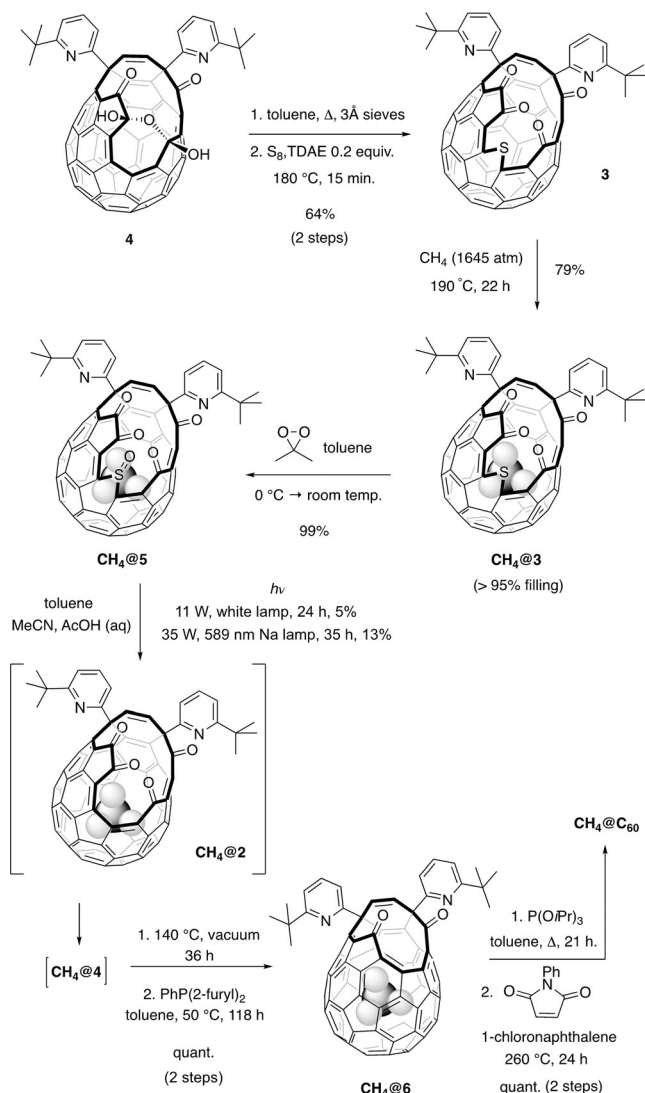
[\*] Dr. S. Bloodworth, G. Sitinova, S. Alom, Dr. S. Vidal, G. R. Bacanu, Dr. S. J. Elliott, Dr. M. E. Light, J. M. Herniman, Prof. G. J. Langley, Prof. M. H. Levitt, Prof. R. J. Whitby  
Chemistry, Faculty of Engineering and Physical Sciences  
University of Southampton  
Southampton, SO17 1BJ (UK)  
E-mail: rjw1@soton.ac.uk  
Dr. S. J. Elliott  
Current address: Centre de Résonance Magnétique Nucléaire à Très Hauts Champs, FRE 2034 Université de Lyon, CNRS, Université Claude Bernard Lyon 1, ENS de Lyon  
5 Rue de la Doua, 69100 Villeurbanne (France)

Supporting information and the ORCID identification number(s) for the author(s) of this article can be found under:  
<https://doi.org/10.1002/anie.201900983>.

© 2019 The Authors. Published by Wiley-VCH Verlag GmbH & Co. KGaA. This is an open access article under the terms of the Creative Commons Attribution License, which permits use, distribution and reproduction in any medium, provided the original work is properly cited.

ism,<sup>[24,31–33]</sup> in which only certain combinations of nuclear spin states and molecular rotational states are allowed by the Pauli principle. We are particularly interested in  $\text{CH}_4@C_{60}$ , since spin isomerism is also exhibited by methane, which exists as three nuclear spin isomers with the  $J=0$  rotational state having nuclear spin  $I=2$ , the  $J=1$  rotational state having nuclear spin  $I=1$ , and the  $J=2$  rotational state having nuclear spin states  $I=0$  and  $I=1$ .<sup>[34,35]</sup> Methane is one of the largest possible guests for  $C_{60}$ <sup>[36]</sup> and herein, we report conditions for optimized  $\text{CH}_4$  encapsulation by **3** and the first successful closure sequence to reform the pristine  $C_{60}$  cage. Our work constitutes the first synthesis of  $\text{CH}_4@C_{60}$  and raises the exciting prospect of accessing other endohedral fullerenes,  $A@C_{60}$ , in which the endohedral species is a “large” guest molecule; including  $A=\text{O}_2$ ,  $\text{N}_2$ ,  $\text{CO}$ ,  $\text{NO}$ ,  $\text{NH}_3$ ,  $\text{CH}_3\text{OH}$ ,  $\text{CH}_2\text{O}$ , and  $\text{CO}_2$ , as well as the atoms Ar and Kr.

$\text{CH}_4@C_{60}$  was prepared according to the procedures shown in Scheme 1. Open-cage fullerene **3** was obtained



**Scheme 1.** Synthesis of  $\text{CH}_4@C_{60}$ . Optimized  $\text{CH}_4$  encapsulation by **3** and a successful closure sequence, involving photochemical desulfinylation, are applied to the first synthesis of  $\text{CH}_4@C_{60}$ .

from bis(hemiketal) **4**<sup>[15]</sup> according to the published method.<sup>[25]</sup> We have previously shown the 17-membered orifice of **3** to be suitable for entry of a single molecule of methane, achieving 65 % encapsulation by heating **3** at 200 °C under 153 atm of methane.<sup>[28]</sup> Upon increasing the pressure of methane above 1500 atm, we obtained  $\text{CH}_4@3$  with more than 95 % encapsulation of methane (estimated from the  $^1\text{H}$  NMR spectrum) after 22 h at 190 °C. Oxidation with dimethyldioxirane<sup>[37]</sup> gave the sulfoxide  $\text{CH}_4@5$  cleanly. Photochemical removal of the sulfinyl group (SO) has been reported for ring-contraction of the sulfoxide derivative of open-cage fullerene **1**, using visible-light irradiation.<sup>[13,38–40]</sup> Unfortunately, Murata and co-workers found that the sulfoxide derivative of **3** (i.e. **5**) does not undergo simple loss of SO under the same conditions, but undergoes decomposition accompanied by a low-yielding rearrangement to a lactone side product.<sup>[41]</sup> However, we noted that the dominant species in the positive-ion atmospheric pressure photoionization (APPI) mass spectrum of **5** appears at  $m/z=1102.18$  and corresponds to the radical cation  $\text{C}_{82}\text{H}_{26}\text{N}_2\text{O}_4^{+\cdot}$  resulting from loss of SO from **5**, indicating that ring-contraction by photochemical removal of SO is feasible. Since we found that the expected product **2** from the photochemical ring-contraction is unstable under visible light irradiation, we considered that the reaction might be facilitated if **2** could be trapped in situ as the bis(hemiketal) **4**. We were pleased to observe that in a mixed solvent system of toluene, acetonitrile, and acetic acid (10 % v/v aq.), irradiation of sulfoxide **5** (containing endohedral water under the partly aqueous reaction conditions), in the visible range for 24 h with an 11 W bulb, gave a mixture of **4** and  $\text{H}_2\text{O}@4$  in 25 % yield of isolated product, with a similar amount of unreacted **5** remaining. A longer period of irradiation did not lead to a higher yield of **4**. Product(s) of polymerization or decomposition, which were not identified, accounted for the remaining material, and none of the lactone product recovered by Murata et al. was isolated.

When  $\text{CH}_4@5$  was subjected to identical photochemical conditions, the corresponding product of SO loss followed by hydration,  $\text{CH}_4@4$ , was obtained in only 5 % yield, retaining more than 95 % methane filling. We confirmed that the observed drop in yield is due to the presence of endohedral methane by carrying out photolysis on a sample of  $\text{CH}_4@5$  with 83 % filling (Supporting Information, Section S5), from which the product  $\text{CH}_4@4$  was obtained with only 57 % filling as a result of the much higher-yielding conversion of the portion of the material that does not contain methane.

The yield of the photochemical ring-contraction was significantly increased upon switching to irradiation with monochromatic (yellow) light at 589 nm, using a low-pressure sodium lamp. A mixture of **5** and  $\text{H}_2\text{O}@5$  was converted to the bis(hemiketal) mixture (**4** +  $\text{H}_2\text{O}@4$ ) in 43 % yield of isolated product. The corresponding reaction of  $\text{CH}_4@5$  under irradiation at 589 nm gave  $\text{CH}_4@4$  in a yield of 13 %, in accordance with the expected inhibition of the reaction by endohedral methane, and is a valuable improvement in comparison with the very low yield obtained using white light. It is rare for endohedral species to affect the reactivity of the fullerene cage,<sup>[42,43]</sup> particularly in such a dramatic (and unfortunate) fashion, but while it is disappointing that this step remains

low-yielding, with CH<sub>4</sub>@4 in hand we were now able to adapt known procedures for suturing of the bis(hemiketal) orifice to an intact C<sub>60</sub> shell.

CH<sub>4</sub>@4 (more than 95 % filling) was contaminated by a trace of H<sub>2</sub>O@4, identified by the <sup>1</sup>H NMR resonance of endohedral water at  $\delta = -9.84$  ppm<sup>[16]</sup> and distinct from the <sup>1</sup>H resonance for endohedral methane in CH<sub>4</sub>@4, which appears as a sharp singlet at  $\delta = -11.22$  ppm (CDCl<sub>3</sub>). Since the percentage filling of H<sub>2</sub>O will be amplified by a factor of approximately five during photochemical ring contraction (Supporting Information, Section S5.1), we extrapolate the methane filling in CH<sub>4</sub>@5 to be more than 99.5 %. To avoid final contamination of CH<sub>4</sub>@C<sub>60</sub> by H<sub>2</sub>O@C<sub>60</sub>, CH<sub>4</sub>@4 was heated at 140 °C under a dynamic vacuum (approximately 0.5 mm Hg) for 36 h to obtain CH<sub>4</sub>@2 with accompanying removal of the endohedral water contaminant. No loss of CH<sub>4</sub> was observed. Subsequent reduction to CH<sub>4</sub>@6 using di-(2-furyl)phenylphosphine in toluene, at a temperature of 50 °C (too low for water re-entry), gave CH<sub>4</sub>@6 (more than 95 % filling) in quantitative yield. Endohedral methane appears as a singlet with a shift of  $\delta_{\text{H}} = -9.82$  ppm (700 MHz, [D<sub>8</sub>]THF, 295 K) in the <sup>1</sup>H NMR spectrum of CH<sub>4</sub>@6, and no H<sub>2</sub>O@6 was present. Finally, the orifice of CH<sub>4</sub>@6 was sutured, using identical conditions to those reported for H<sub>2</sub>O@6,<sup>[16]</sup> and CH<sub>4</sub>@C<sub>60</sub> was obtained with 100.0 ± 0.3 % filling after removal of traces of (empty) C<sub>60</sub> by preparative HPLC on a Cosmosil™ Buckyprep column. An independently prepared sample of H<sub>2</sub>O@C<sub>60</sub> was found to co-elute with CH<sub>4</sub>@C<sub>60</sub>, confirming the necessity for removal of contaminant endohedral water earlier in the synthesis.

The positive-ion APPI mass spectrum of CH<sub>4</sub>@C<sub>60</sub> is in agreement with the calculated isotope distribution pattern for C<sub>61</sub>H<sub>4</sub> (Figure 2), and the ultrahigh resolution also confirms that H<sub>2</sub>O@C<sub>60</sub> is not present since the isotope patterns for CH<sub>4</sub>@C<sub>60</sub> and H<sub>2</sub>O@C<sub>60</sub> were shown to be non-overlapping (Supporting Information, Section S4).

A crystal structure of the nickel(II) octaethylporphyrin/benzene solvate<sup>[44]</sup> of CH<sub>4</sub>@C<sub>60</sub> was obtained (CCDC 1858399 contain the supplementary crystallographic data for this paper. These data can be obtained free of charge from The Cambridge Crystallographic Data Centre.) and is similar to that reported for the equivalent C<sub>60</sub> solvate,<sup>[45]</sup> with the

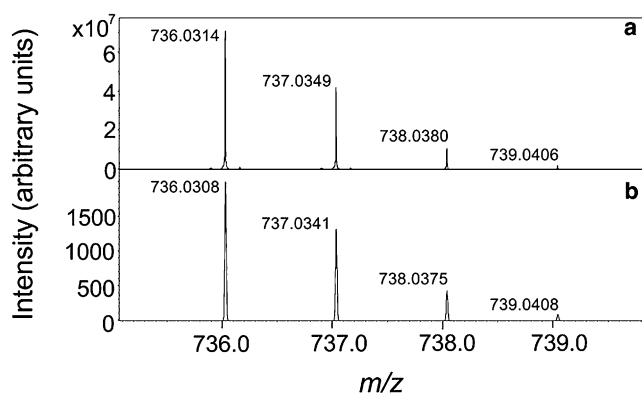


**Figure 2.** Positive-ion APPI mass spectrum of CH<sub>4</sub>@C<sub>60</sub>. a) Experimental data and b) model isotope pattern for C<sub>61</sub>H<sub>4</sub>; *m/z* 735–740.

exception of a spherically symmetrical electron density distribution located at the center of the fullerene, corresponding to the endohedral methane molecule. The electron density map shows a faint spherical shell around the main center of the endohedral electron density, at a radius of 1.03 Å (Figure 3). This shell of distributed electron density corre-

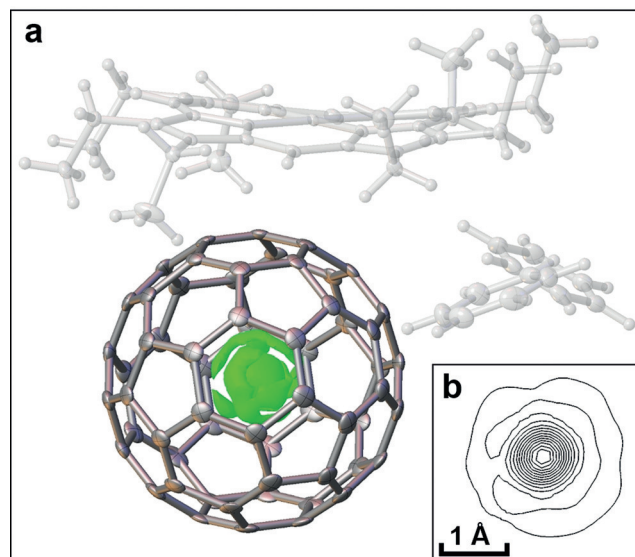


**Figure 3.** Crystal structure for the nickel(II) octaethylporphyrin/benzene solvate of CH<sub>4</sub>@C<sub>60</sub>. a) Thermal ellipsoids for the cage atoms of CH<sub>4</sub>@C<sub>60</sub> and the difference electron density map for endohedral CH<sub>4</sub> (surface drawn at the 0.6 e Å<sup>3</sup> level) are shown. Ni<sup>II</sup>OEP and benzene are shown as thermal ellipsoids in white and all thermal ellipsoids are shown at 50% probability. b) Selected slice through the center of difference electron density at the CH<sub>4</sub> position, contours drawn at approximately 0.9 e Å<sup>3</sup>. A faint shell of electron density at a radius of 1.03 Å from the center of the cage is visible. This corresponds to the delocalized wavefunction of the methane hydrogen atoms. CCDC 1858399 contain the supplementary crystallographic data for this paper. These data can be obtained free of charge from The Cambridge Crystallographic Data Centre. Structure details are reported in Section S6 of the Supporting Information.

sponds to the delocalized nuclear wavefunction of the methane hydrogens, as expected for a quantum description of the freely rotating molecule. This quantum description is well-established for the analogous systems H<sub>2</sub>@C<sub>60</sub>, H<sub>2</sub>O@C<sub>60</sub>, and HF@C<sub>60</sub>, which have been extensively studied by neutron-scattering and infrared spectroscopy.<sup>[17,20–22]</sup> A classical description in which the methane explores a random set of orientations would give a similar result. There is no geometrical evidence (within 3-sigma) for distortion of the cage relative to the C<sub>60</sub> analogue, or displacement of the methane from its center.

Detailed NMR characterization of CH<sub>4</sub>@C<sub>60</sub> was carried out. The <sup>1</sup>H NMR spectrum in 1,2-dichlorobenzene-*d*<sub>4</sub> displays a singlet at  $\delta_{\text{H}} = -5.71$  ppm, where the shift results from the shielding effect of the C<sub>60</sub> cage, compared with <sup>12</sup>CH<sub>4</sub> in the gas phase, which has a chemical shift of  $\delta_{\text{H}} = 2.166 \pm 0.002$  ppm.<sup>[46]</sup> From the natural abundance <sup>13</sup>CH<sub>4</sub>@C<sub>60</sub>, the measured coupling is <sup>1</sup>J<sub>HC</sub> = 124.3 ± 0.2 Hz (at 295 K), in comparison with <sup>1</sup>J<sub>HC</sub> = 125.3 Hz (at 292 K) measured in the



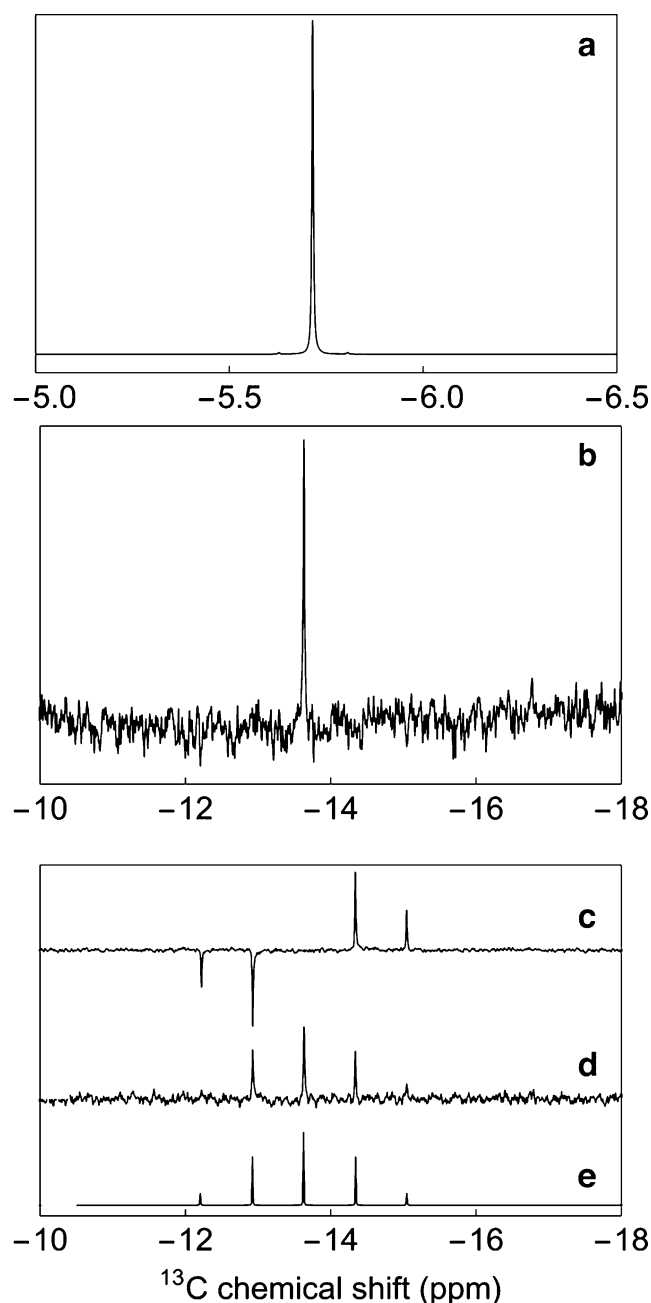
gas phase.<sup>[47]</sup> The liquid state  $^{13}\text{C}\{^1\text{H}\}$  NMR spectrum reports a sharp singlet for endohedral methane at  $\delta_{\text{C}} = -13.63$  ppm in 1,2-dichlorobenzene- $d_4$ , again shielded in comparison with the reported shift of  $\delta_{\text{C}} = -8.648 \pm 0.001$  ppm measured in the gas phase<sup>[46]</sup> (Figure 4 a,b).

Figure 4c,d shows the relevant section of the INEPT NMR spectrum of  $^{13}\text{CH}_4@C_{60}$ , alongside experimental and simulated proton-coupled  $^{13}\text{C}$  NMR spectra. The INEPT pulse sequence was used as defined by Morris and Freeman<sup>[48]</sup> with an interpulse delay of  $\tau = \frac{1}{4J_{\text{HC}}} = 2.012$  ms ( $J_{\text{HC}} = 124.3$  Hz). The experimental  $^{13}\text{C}$  resonance is a 1:4:6:4:1 quintet with chemical shift  $\delta_{\text{C}} = -13.63$  ppm. The  $^{13}\text{C}$  NMR resonance for the cage in  $\text{CH}_4@C_{60}$  appears at  $\delta_{\text{C}} = 143.20$  ppm, shifted by  $\Delta\delta = +0.52$  ppm relative to  $C_{60}$  itself. This is a large deshielded shift of the cage  $^{13}\text{C}$  NMR resonance in comparison with the effect of smaller molecular endohedral species ( $\text{HF}@C_{60}$ ,  $\Delta\delta = +0.04$  ppm,<sup>[17]</sup>  $\text{H}_2@C_{60}$ ,  $\Delta\delta = +0.08$  ppm,<sup>[16]</sup> and  $\text{H}_2\text{O}@C_{60}$ ,  $\Delta\delta = +0.11$  ppm<sup>[15,16]</sup>), consistent with the large size of methane. Correlation of  $\Delta\delta$  with the van der Waals radius of the enclosed species has been described for the inert  $\text{gas}@C_{60}$  series.<sup>[49]</sup>

The  $^1\text{H}$  spin-lattice relaxation time constant of  $^{12}\text{CH}_4@C_{60}$  was found to be  $T_1 = 1.4904 \pm 0.0005$  s at 295 K. Measurement of  $T_1$  as a function of temperature indicates a clear increase in relaxation rate constant ( $T_1^{-1}$ ) with increasing temperature. This is indicative of a significant spin-rotation contribution to the relaxation, and is consistent with  $^1\text{H}$  relaxation of methane in the gas phase<sup>[51]</sup> (Figure 5 a).

The  $^{13}\text{C}$   $T_1$  values for endohedral methane, reported by the  $^{13}\text{C}$  satellites of the  $^1\text{H}$  spectrum using a modified INEPT sequence (Supporting Information, Section S3.2), are slightly different:  $T_1 = 0.39 \pm 0.14$  s for the less shielded satellite, and  $T_1 = 0.55 \pm 0.14$  s for the more shielded satellite (Figure 5 b). This difference is likely to be associated with cross-correlated relaxation effects.<sup>[52]</sup>

In summary,  $\text{CH}_4@C_{60}$ , the first example of an organic molecule trapped in  $C_{60}$ , has been synthesized.  $\text{CH}_4$  is the largest molecule, with the greatest number of atoms, to have been encapsulated in  $C_{60}$  to date. The first step of the orifice contraction was strongly inhibited by the presence of endohedral methane, resulting in a low yield for the key photolytic step.  $\text{CH}_4@C_{60}$  was characterized by high resolution mass spectrometry, NMR spectroscopy, and X-ray crystallography.  $^1\text{H}$  spin-lattice relaxation times for endohedral methane are similar to those observed in the gas phase, providing evidence that methane is freely rotating inside the  $C_{60}$  cage. The experimental  $^{13}\text{C}$  NMR chemical shift of the cage carbon is shifted by  $+0.52$  ppm relative to empty  $C_{60}$ . We find no evidence for distortion of the cage from a crystal structure of the nickel(II) octaethylporphyrin/ benzene solvate of  $\text{CH}_4@C_{60}$ . In the crystal structure, the hydrogen atoms of methane appear as a spherically symmetric sphere of electron density, consistent with a delocalized quantum state. Neutron scattering, infrared spectroscopy, and cryogenic NMR spectroscopy experiments are now planned to study spin-isomerism and spin-isomer conversion of the encapsulated methane molecules. The successful synthesis of  $\text{CH}_4@C_{60}$  opens a route to novel endofullerenes  $\text{A}@C_{60}$  enclosing "large" endohedral species A, such as  $\text{A} = \text{O}_2$ ,



**Figure 4.**  $^1\text{H}$  and  $^{13}\text{C}$  NMR resonances for endohedral methane in  $\text{CH}_4@C_{60}$ . a) Experimental  $^1\text{H}$  NMR resonance of  $\text{CH}_4@C_{60}$  acquired with 1 transient, b) Experimental  $^{13}\text{C}$  NMR resonance of  $\text{CH}_4@C_{60}$  with  $^1\text{H}$  WALTZ16 decoupling (nutration frequency = 14.2 kHz), acquired with 4928 transients and a delay of 10 s between scans, c) Experimental non-proton-decoupled  $^{13}\text{C}$  INEPT spectrum, acquired with 35 840 transients and a delay of 4.5 s between scans, d) Experimental non-proton-decoupled  $^{13}\text{C}$  NMR spectrum excited by a single  $90^\circ$  pulse, acquired with 35 840 transients and a delay of 4.5 s between scans, e) Numerical simulation of (d) using *SpinDynamica*.<sup>[50]</sup> All experimental spectra were acquired for a degassed 4.5 mm sample of  $\text{CH}_4@C_{60}$  in 1,2-dichlorobenzene- $d_4$  at 16.45 T ( $^1\text{H}$  nuclear Larmor frequency = 700 MHz and  $^{13}\text{C}$  nuclear Larmor frequency = 176 MHz) and 295 K.

$\text{NO}$ ,  $\text{NH}_3$ ,  $\text{N}_2$ ,  $\text{CO}_2$ ,  $\text{CH}_3\text{OH}$ , and  $\text{H}_2\text{CO}$ , with exciting prospects for the study of these encapsulated small molecules.

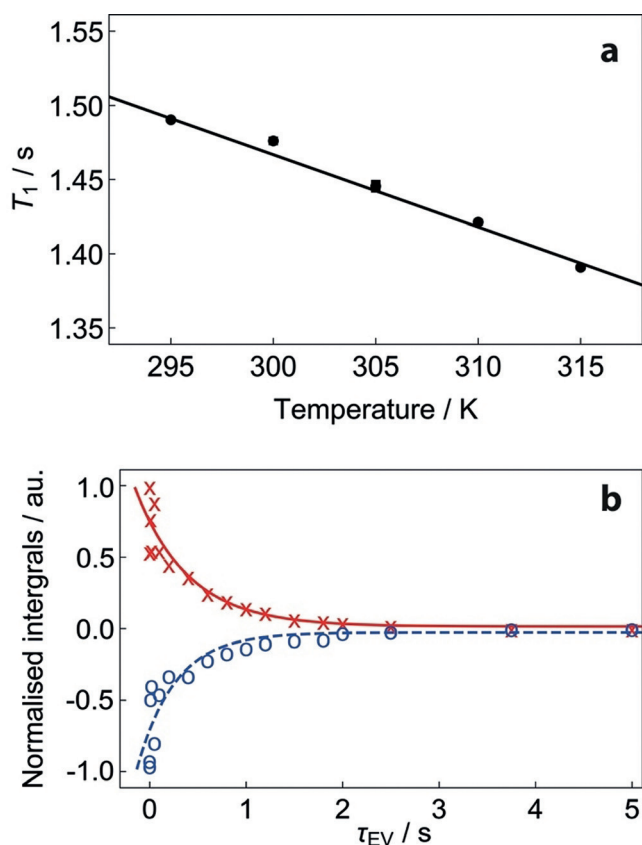


**Figure 5.** Experimental  $^1\text{H}$  and  $^{13}\text{C}$  spin-lattice relaxation times for endohedral methane in  $\text{CH}_4@C_{60}$ . a) Experimental  $^1\text{H}$  spin lattice relaxation as a function of temperature for  $^{12}\text{CH}_4@C_{60}$ . The best straight-line fit to the experimental data points is shown.  $^1\text{H}$  longitudinal relaxation times were measured using the inversion-recovery pulse sequence; b) Experimental  $^{13}\text{C}$  spin-lattice relaxation curves for  $^{13}\text{CH}_4@C_{60}$  (natural abundance). Spectra were acquired for a degassed 4.5 mm solution of  $\text{CH}_4@C_{60}$  in 1,2-dichlorobenzene- $d_4$  at 16.45 T ( $^1\text{H}$  nuclear Larmor frequency = 700 MHz) and 295 K. Red data points  $\times$  correspond to the satellite at  $\delta = -5.638$  ppm; Blue data points  $\circ$  correspond to the satellite at  $\delta = -5.815$  ppm. The  $^{13}\text{C}$  longitudinal relaxation time  $T_1$  was measured using the pulse sequence described in Section S3.2 of the Supporting Information. All signal amplitudes were normalized to the maximum integral (second data point,  $\tau_{\text{EV}} = 1$  ms). The fitted curves have single exponential form.

### Experimental Section

Details of the synthesis and characterization of  $\text{CH}_4@C_{60}$  are in the Supporting Information. Original data may be found at <https://doi.org/10.5258/SOTON/D0809>.

### Acknowledgements

This work was supported by the Engineering and Physical Sciences Research Council (EP/M001962/1, EP/P009980/1), including core capability (EP/K039466), and the European Research Council (786707-FunMagResBeacons).

### Conflict of interest

The authors declare no conflict of interest.

**Keywords:** endohedral fullerene · mass spectrometry · NMR spectroscopy · synthetic methods · X-ray diffraction

**How to cite:** *Angew. Chem. Int. Ed.* **2019**, *58*, 5038–5043  
*Angew. Chem.* **2019**, *131*, 5092–5097

- [1] H. W. Kroto, J. R. Heath, S. C. O'Brien, R. F. Curl, R. E. Smalley, *Nature* **1985**, *318*, 162–163.
- [2] J. R. Heath, S. C. O'Brien, Q. Zhang, Y. Liu, R. F. Curl, H. W. Kroto, F. K. Tittel, R. E. Smalley, *J. Am. Chem. Soc.* **1985**, *107*, 7779–7780.
- [3] X. Lu, L. Feng, T. Akasaka, S. Nagase, *Chem. Soc. Rev.* **2012**, *41*, 7723–7760.
- [4] A. A. Popov, *Nanostruct. Sci. Technol.* **2017**, 1–34.
- [5] A. A. Popov, S. F. Yang, L. Dunsch, *Chem. Rev.* **2013**, *113*, 5989–6113.
- [6] S. Osuna, M. Swart, M. Sola, *Chem. Eur. J.* **2009**, *15*, 13111–13123.
- [7] M. Saunders, R. J. Cross, H. A. Jiménez-Vázquez, R. Shimshi, A. Khong, *Science* **1996**, *271*, 1693–1697.
- [8] T. Almeida Murphy, T. Pawlik, A. Weidinger, M. Hohne, R. Alcalá, J. M. Spaeth, *Phys. Rev. Lett.* **1996**, *77*, 1075–1078.
- [9] S. C. Chuang, F. R. Clemente, S. I. Khan, K. N. Houk, Y. Rubin, *Org. Lett.* **2006**, *8*, 4525–4528.
- [10] Y. Rubin, *Chem. Eur. J.* **1997**, *3*, 1009–1016.
- [11] Y. Rubin, T. Jarrosson, G. W. Wang, M. D. Bartberger, K. N. Houk, G. Schick, M. Saunders, R. J. Cross, *Angew. Chem. Int. Ed.* **2001**, *40*, 1543–1546; *Angew. Chem.* **2001**, *113*, 1591–1594.
- [12] G. Schick, T. Jarrosson, Y. Rubin, *Angew. Chem. Int. Ed.* **1999**, *38*, 2360–2363; *Angew. Chem.* **1999**, *111*, 2508–2512.
- [13] K. Komatsu, M. Murata, Y. Murata, *Science* **2005**, *307*, 238–240.
- [14] Y. Murata, M. Murata, K. Komatsu, *J. Am. Chem. Soc.* **2003**, *125*, 7152–7153.
- [15] K. Kurotobi, Y. Murata, *Science* **2011**, *333*, 613–616.
- [16] A. Krachmalnicoff, M. H. Levitt, R. J. Whitby, *Chem. Commun.* **2014**, *50*, 13037–13040.
- [17] A. Krachmalnicoff, et al., *Nat. Chem.* **2016**, *8*, 953–957.
- [18] A. Krachmalnicoff, R. Bounds, S. Mamone, M. H. Levitt, M. Carravetta, R. J. Whitby, *Chem. Commun.* **2015**, *51*, 4993–4996.
- [19] M. H. Levitt, *Philos. Trans. R. Soc. London Ser. A* **2013**, *371*, 20120429.
- [20] C. Beduz, et al., *Proc. Natl. Acad. Sci. USA* **2012**, *109*, 12894–12898.
- [21] S. Mamone, et al., *J. Chem. Phys.* **2009**, *130*, 081103.
- [22] S. Mamone, M. Jiménez-Ruiz, M. R. Johnson, S. Rols, A. J. Horsewill, *Phys. Chem. Chem. Phys.* **2016**, *18*, 29369–29380.
- [23] M. Z. Xu, F. Sebastianelli, B. R. Gibbons, Z. Bacic, R. Lawler, N. J. Turro, *J. Chem. Phys.* **2009**, *130*, 224306.
- [24] B. Meier, S. Mamone, M. Concistrè, J. Alonso-Valdesueiro, A. Krachmalnicoff, R. J. Whitby, *Nat. Commun.* **2015**, *6*, 8112.
- [25] T. Futagoishi, M. Murata, A. Wakamiya, T. Sasamori, Y. Murata, *Org. Lett.* **2013**, *15*, 2750–2753.
- [26] T. Futagoishi, M. Murata, A. Wakamiya, Y. Murata, *Angew. Chem. Int. Ed.* **2015**, *54*, 14791–14794; *Angew. Chem.* **2015**, *127*, 15004–15007.
- [27] T. Futagoishi, M. Murata, A. Wakamiya, Y. Murata, *Angew. Chem. Int. Ed.* **2017**, *56*, 2758–2762; *Angew. Chem.* **2017**, *129*, 2802–2806.
- [28] S. Bloodworth, et al., *ChemPhysChem* **2018**, *19*, 266–276.
- [29] S. Hasegawa, Y. Hashikawa, T. Kato, Y. Murata, *Angew. Chem. Int. Ed.* **2018**, *57*, 12804–12808; *Angew. Chem.* **2018**, *130*, 12986–12990.

- [30] T. Futagoishi, T. Aharen, T. Kato, A. Kato, T. Ihara, T. Tada, M. Murata, A. Wakamiya, H. Kageyama, Y. Kanemitsu, Y. Murata, *Angew. Chem. Int. Ed.* **2017**, *56*, 4261–4265; *Angew. Chem.* **2017**, *129*, 4325–4329.
- [31] S. Mamone, et al., *J. Chem. Phys.* **2014**, *140*, 194306.
- [32] B. Meier, K. Kouřil, C. Bengs, H. Kouřilova, T. C. Barker, S. J. Elliott, S. Alom, R. J. Whitby, M. H. Levitt, *Phys. Rev. Lett.* **2018**, *120*, 266001.
- [33] N. J. Turro, A. A. Martí, J. Y.-C. Chen, S. Jockusch, R. G. Lawler, M. Ruzzi, E. Sartori, S. C. Chuang, K. Komatsu, Y. Murata, *J. Am. Chem. Soc.* **2008**, *130*, 10506–10507.
- [34] P. Cacciani, J. Cosleou, M. Khelkhal, P. Cermak, C. Puzzarini, *J. Phys. Chem. A* **2016**, *120*, 173–182.
- [35] T. Sugimoto, K. Yamakawa, I. Arakawa, *J. Chem. Phys.* **2015**, *143*, 224305.
- [36] K. E. Whitener, R. J. Cross, M. Saunders, S. Iwamatsu, S. Murata, N. Mizorogi, S. Nagase, *J. Am. Chem. Soc.* **2009**, *131*, 6338–6339.
- [37] W. Adam, J. Bialas, L. Hadjiarapoglou, *Chem. Ber.* **1991**, *124*, 2377–2377.
- [38] Y. Morinaka, F. Tanabe, M. Murata, Y. Murata, K. Komatsu, *Chem. Commun.* **2010**, *46*, 4532–4534.
- [39] M. Murata, S. Maeda, Y. Morinaka, Y. Murata, K. Komatsu, *J. Am. Chem. Soc.* **2008**, *130*, 15800–15801.
- [40] M. Murata, Y. Murata, K. Komatsu, *J. Am. Chem. Soc.* **2006**, *128*, 8024–8033.
- [41] T. Futagoishi, M. Murata, A. Wakamiya, Y. Murata, *Chem. Commun.* **2017**, *53*, 1712–1714.
- [42] E. E. Maroto, J. Mateos, M. García-Borràs, S. Osuna, S. Filippone, M. A. Herranz, Y. Murata, M. Solà, N. Martín, *J. Am. Chem. Soc.* **2015**, *137*, 1190–1197.
- [43] S. Vidal, M. Izquierdo, S. Alom, M. García-Borràs, S. Filippone, S. Osuna, M. Solà, R. J. Whitby, N. Martín, *Chem. Commun.* **2017**, *53*, 10993–10996.
- [44] M. M. Olmstead, D. A. Costa, K. Maitra, B. C. Noll, S. L. Phillips, P. M. van Calcar, A. L. Balch, *J. Am. Chem. Soc.* **1999**, *121*, 7090–7097.
- [45] H. M. Lee, M. M. Olmstead, T. Suetsuna, H. Shimotani, N. Drago, R. J. Cross, K. Kitazawa, A. L. Balch, *Chem. Commun.* **2002**, 1352–1353.
- [46] A. Antušek, K. Jackowski, M. Jaszunski, W. Makulski, M. Wilczek, *Chem. Phys. Lett.* **2005**, *411*, 111–116.
- [47] B. Bennett, W. T. Raynes, *Mol. Phys.* **1987**, *61*, 1423–1430.
- [48] G. A. Morris, R. Freeman, *J. Am. Chem. Soc.* **1979**, *101*, 760–762.
- [49] R. G. Lawler, *Nanostruct. Sci. Technol.* **2017**, 229–263.
- [50] C. Bengs, M. H. Levitt, *Magn. Reson. Chem.* **2018**, *56*, 374–414.
- [51] C. J. Jameson, A. K. Jameson, N. C. Smith, J. K. Hwang, T. N. Zia, *J. Phys. Chem.* **1991**, *95*, 1092–1098.
- [52] A. Kumar, R. C. R. Grace, P. K. Madhu, *Prog. Nucl. Magn. Reson. Spectrosc.* **2000**, *37*, 191–319.

Manuscript received: January 24, 2019

Accepted manuscript online: February 18, 2019

Version of record online: March 12, 2019